

Effects of radiation on unsteady three-dimensional boundary layer flow and heat transfer over a permeable axisymmetric shrinking sheet with suction

Dinesh Rajotia*

Department of Mathematics, University of Rajasthan, Jaipur 302 004, India

Received 28 July 2015; accepted 7 January 2018

In the present analysis, we have investigated the effects of thermal radiation on an unsteady three-dimensional boundary layer flow of an incompressible viscous fluid and heat transfer due to a permeable axisymmetric shrinking sheet with suction and power-law variation in wall temperature. The similarity transformations have been used to convert the governing partial differential equations into non-linear ordinary differential equations and then solved numerically by shooting technique. The conditions of the existence, non-existence and duality of the similarity solution have been explored by the investigation where the solution depends not only on suction parameter but on unsteadiness parameter also. Further, it has been emerged that the range of the suction parameter S , where the similarity solution exists, is increased with the increase of unsteadiness parameter A . Also, the graphs of velocity profile, temperature profile, skin-friction coefficient and rate of heat transfer at the sheet have been drawn with various values of the parameters and then discussed these characteristic features in detail.

Keywords: Unsteady boundary layer flow, Axisymmetric shrinking sheet, Radiation effect, Suction

1 Introduction

The viscous flow over a stretching/shrinking sheet has enamours applications in engineering processes such as glass-fiber production, wire drawing, paper production and extraction of polymer sheets etc. Crane¹ was the first who investigated the steady viscous flow of an incompressible fluid over a linearly stretching sheet and gave a closed analytical similarity solution. Gupta and Gupta² studied the heat and mass transfer problem in Newtonian boundary layer flow due to a stretching sheet with suction and blowing. A steady three-dimensional flow of viscous fluid over a plane surface which was stretched in its own plane in two lateral directions at different rates was considered by Wang³. Further, Ariel⁴ gave generalized 3D flow due to a stretching sheet. Three dimensional flow over a stretching surface with thermal radiation and heat generation in the presence of the chemical reaction and suction/injunction was studied by Elbashbeshy *et al.*⁵. Recently, MHD stagnation point flow and heat transfer of a micropolar fluid over a stretching sheet was investigated by Jat *et al.*⁶. Again, Jat *et al.*⁷ studied MHD boundary layer flow and heat and mass transfer for viscous flow over nonlinearly stretching sheet in a porous medium.

Recently, the flow induced by a shrinking sheet has attracted more considerable interest due to its quite distinct physical phenomena in comparison with the flow due to the stretching sheet. On the shrinking sheet, a steady boundary layer flow is not possible unless the vorticity generated in this case is confined within the boundary layer. Therefore, the flow needs a certain amount of external suction at the porous sheet to maintain the boundary layer structure. First of all, Wang⁸ found the concept of flow due to a shrinking sheet while investigating the behaviour of liquid film on the unsteady stretching sheet. Consequently, Miklavcic and Wang⁹ investigated both two-dimensional and axisymmetric flow due to a shrinking sheet in the presence of uniform suction and approved that the existence of the similarity solution is only possible in a certain range of suction parameter. The 2D as well as axisymmetric stagnation-point flow towards a shrinking sheet was considered by Wang¹⁰. Muhaimin and Khamis¹¹ studied the effects of heat and mass transfer on nonlinear MHD boundary layer flow over a shrinking sheet in the presence of suction. A series solution of three-dimensional MHD and rotating flow over a shrinking sheet with suction was obtained by Hayat *et al.*¹². Fang and Zhang¹³ obtained an analytical solution of thermal boundary layer flow over a shrinking sheet. Bhattacharyya¹⁴ gave the effects of radiation and heat source/sink on unsteady MHD boundary layer flow and heat transfer over a

*E-mail: rajotia.dinesh@gmail.com

shrinking sheet with suction/injection. Bhattacharyya and Layek¹⁵ studied the stagnation-point flow and heat transfer towards a shrinking sheet with thermal radiation and Suction. While, the axisymmetric stagnation flow over axisymmetric shrinking sheet is taken by Rajotia and Jat¹⁶. Further, Jat and Rajotia¹⁷ studied dual solutions of MHD flow and heat transfer over a shrinking sheet with variable wall temperature and then slip flow past an nonlinearly shrinking sheet investigated by Ghosh *et al.*¹⁸. Recently, Casson fluid flow with variable wall temperature and thermal radiation was taken by Bhattacharyya *et al.*¹⁹. Consequently, dual nature study of thermophysical effects of water driven nanoparticles on MHD axisymmetric permeable shrinking sheet was considered by Haq *et al.*²⁰ and then, Ghosh and Mukhopadhyay²¹ observed the flow of nanofluid due to exponentially shrinking sheet.

In the above investigation only steady state condition is considered. However, in some conditions, the flow becomes time dependent and it is necessary to consider the flow of unsteadiness. Devi *et al.*²² studied the unsteady three-dimensional boundary flow with heat and mass transfer due to a stretching surface. Mukhopadhyay and Anderson²³ investigated slip effects on unsteady two dimensional flow and heat transfer over a stretching sheet. Then, radiative effect on the flow and heat transfer over an unsteady stretching sheet was given by Abd El-Aziz²⁴. The viscous flow over an unsteady shrinking sheet with mass transfer was studied by Fang *et al.*²⁵ and obtained multiple branch solutions in a certain range of mass suction and unsteadiness parameters. Bachok *et al.*²⁶ considered an unsteady 3D flow due to a permeable shrinking sheet. Further, Chamkha *et al.*²⁷ analyzed the effects of chemical reaction on unsteady free convective heat and mass transfer on a porous stretching surface in a porous medium. Consequently, unsteady Casson fluid flow over non-linear stretching sheet was considered by Ullah *et al.*²⁸. Recently, Aurangzaib *et al.*²⁹ investigated the effect of partial slip of unsteady MHD stagnation flow of micropolar fluid over the shrinking sheet.

However, in the above analysis, the effects of radiation on unsteady three-dimensional boundary layer flow past a shrinking sheet are not studied yet. Therefore, in the present analysis, we are investigating the effects of unsteadiness parameter with thermal radiation on 3D boundary layer flow and heat transfer due a permeable axisymmetric shrinking sheet with suction and power-law variation in wall temperature.

2 Formulation of Problem

Consider an unsteady three dimensional boundary layer flow of an incompressible viscous fluid and heat transfer due to a permeable sheet which shrinks into two lateral directions with the same rate in its own plane (Fig. 1). The velocity components u , v and w are taken along the x , y and z directions, respectively, where the x and y axes are along the length and breadth of the sheet and the z axis is perpendicular to the sheet. On the surface of the sheet, the shrinking velocities with dimension t^{-1} are:

$$u = U(x, t) = -ax/(1-\alpha t),$$

$$v = V(y, t) = -ay/(1-\alpha t),$$

where $a(> 0)$ is the shrinking constant and $\alpha (> 0)$ is a constant.

Under the usual boundary layer approximations, the basic governing boundary layer equations of continuity, momentum and heat are given as

$$\frac{\partial u}{\partial x} + \frac{\partial v}{\partial y} + \frac{\partial w}{\partial z} = 0 \quad \dots (1)$$

$$\frac{\partial u}{\partial t} + u \frac{\partial u}{\partial x} + v \frac{\partial u}{\partial y} + w \frac{\partial u}{\partial z} = \nu \frac{\partial^2 u}{\partial z^2} \quad \dots (2)$$

$$\frac{\partial v}{\partial t} + u \frac{\partial v}{\partial x} + v \frac{\partial v}{\partial y} + w \frac{\partial v}{\partial z} = \nu \frac{\partial^2 v}{\partial z^2} \quad \dots (3)$$

$$\frac{\partial T}{\partial t} + u \frac{\partial T}{\partial x} + v \frac{\partial T}{\partial y} + w \frac{\partial T}{\partial z} = \frac{\kappa}{\rho c_p} \frac{\partial^2 T}{\partial z^2} - \frac{1}{\rho c_p} \frac{\partial q_r}{\partial z} \quad \dots (4)$$

where $\nu = \mu/\rho$ is the kinematic viscosity, μ is the dynamic viscosity, ρ is the density of the fluid, T is the temperature, κ is the fluid thermal conductivity, diffusion coefficient, c_p is the specific heat at constant pressure and q_r is the radiative heat flux.

Using Rosseland approximation for radiation (Brewster³⁰), we obtain $q_r = -\left(\frac{4\sigma}{3k}\right)\frac{\partial T^4}{\partial z}$, where σ is the Stefan-Boltzmann constant and k is absorption coefficient. We consider that the temperature

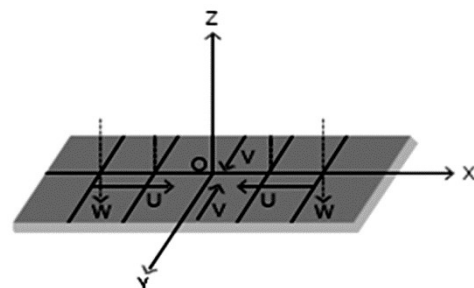


Fig. 1 — Systematic diagram of physical model.

variation within the flow is such that T^4 may be expanded about T_∞ in a Taylor series. Therefore, by neglecting the higher order terms of the series, we get, $T^4 = 4T_\infty^3 T - 3T_\infty^4$. Hence, the Eq. (4) reduces as:

$$\frac{\partial T}{\partial t} + u \frac{\partial T}{\partial x} + v \frac{\partial T}{\partial y} + w \frac{\partial T}{\partial z} = \left(\frac{\kappa}{\rho c_p} + \frac{16\sigma T_\infty^3}{3k\rho c_p} \right) \frac{\partial^2 T}{\partial z^2} \quad \dots (5)$$

The boundary conditions applicable to the present flow are:

$$\begin{aligned} z = 0: u = U(x, t), v = V(y, t), w = \frac{-W}{\sqrt{(1-\alpha t)}}, T = T_w, \\ z \rightarrow \infty: u \rightarrow 0, v \rightarrow 0 \text{ and } T \rightarrow T_\infty \end{aligned} \quad \dots (6)$$

where $W (> 0)$ is the suction velocity in the z -direction, $T_w = T_\infty + T_0(xy)^n/(1-\alpha t)^2$ is the variable surface temperature, $T_0 > 0$ is the constant and n is the power-law exponent signifying the change of amount of heat on the shrinking sheet.

3 Analysis

Introducing the following similarity transformations and dimensionless variables $\eta, f(\eta)$ and $\theta(\eta)$:

$$\begin{aligned} u = \alpha x f'(\eta)/(1-\alpha t), \\ v = \alpha y f'(\eta)/(1-\alpha t), \\ w = -2\sqrt{\alpha\nu} f(\eta)/\sqrt{(1-\alpha t)}, \\ T = T_\infty + (T_w - T_\infty)\theta(\eta), \\ \eta = z\sqrt{\alpha/\nu(1-\alpha t)} \end{aligned} \quad \dots (7)$$

Equation (1) is identically satisfied by similarity transformations, while Eqs (2) and (3) convert into a same Eq. (8) and Eq. (5) becomes as Eq. (9):

$$f''' + 2ff'' - f'^2 - A \left(f' + \frac{\eta}{2} f'' \right) = 0, \quad \dots (8)$$

$$(3R + 4)\theta'' + 6RPr \left[f\theta' - nf'\theta - A \left(\theta + \frac{\eta}{4} \theta' \right) \right] = 0, \quad \dots (9)$$

Corresponding boundary conditions are:

$$\begin{aligned} \eta = 0: f(\eta) = S, f'(\eta) = -1, \theta(\eta) = 1, \\ \eta \rightarrow \infty: f'(\eta) \rightarrow 0, \theta(\eta) \rightarrow 0, \end{aligned} \quad \dots (10)$$

where $A = \alpha/a$ is the unsteadiness parameter, $R = \kappa k/4\sigma T_\infty^3$ is the thermal radiation parameter, $Pr = \mu c_p/\kappa$ is the Prandtl number, $S = W/2\sqrt{\alpha\nu}$ is the suction parameter, and a prime denotes differentiation with respect to similarity variable η .

The skin friction coefficient at the surface of the shrinking sheet is denoted by S_{fx} and S_{fy} along the x and y -directions, respectively, and the rate of heat transfer at the surface of the sheet, i.e., Nusselt number Nu are given as:

$$\begin{aligned} S_{fx} = \tau_{wx}/(\rho U^2/2) = [2/\sqrt{Re_x}] f''(0), \\ S_{fy} = \tau_{wy}/(\rho V^2/2) = [2/\sqrt{Re_y}] f''(0), \\ Nu = -x(\partial T/\partial z)_{z=0}/(T_w - T_\infty) = -\sqrt{Re_x} \theta'(0), \end{aligned}$$

Where $\tau_{wx} = \mu(\partial u/\partial z)_{z=0}$ and $\tau_{wy} = \mu(\partial v/\partial z)_{z=0}$ are the wall shear stresses and $Re_x = \sqrt{\nu(1-\alpha t)}/\alpha x^2 = Ux/\nu$, and $Re_y = \sqrt{\nu(1-\alpha t)}/\alpha y^2 = Vy/\nu$, are the local Reynolds numbers along the x and y -directions, respectively.

4 Numerical Method of Solution

The Boundary value problem (BVP) formed by the set of nonlinear ordinary differential Eqs (8) and (9) along with boundary conditions (10) can be solved numerically by converting it to an initial value problem (IVP) using the shooting technique. We set them into the following system of first order equations:

$$f' = p, p' = q, q' = -2fq + p^2 + A(p + \frac{\eta}{2}q) \quad \dots (11)$$

$$\theta' = r,$$

$$r' = [6RPr/(3R + 4)][-fr + np\theta + A \left(\theta + \frac{\eta}{4}r \right)] \quad \dots (12)$$

With boundary conditions

$$\begin{aligned} f(0) = S, p(0) = -1, \theta(0) = 1, \\ f'(\eta_\infty) = 0, \theta(\eta_\infty) = 0, \end{aligned} \quad \dots (13)$$

In order to integrate the system of Eqs (11) and (12) as an IVP, one requires a value for $q(0)$, i.e., $f'(0)$ and $r(0)$, i.e., $\theta'(0)$ but no such values are given in boundary condition (13). Now, choosing the suitable guesses for $f'(0)$ and $\theta'(0)$ and using the fourth order Runge-Kutta method to solve the IVP, a solution is obtained. Comparing the calculated values of $f'(\eta)$, and $\theta(\eta)$ at $\eta_\infty = 10$ (a suitable finite value of $\eta \rightarrow \infty$ which gives asymptotic approach to all the solutions) with the given boundary conditions $f'(\eta_\infty)$ and $\theta(\eta_\infty)$ and adjusting the estimated values of $f'(0)$ and $\theta'(0)$ using the Secant method to obtain better approximation for the solution. Here, the step-size is taken as $\Delta\eta = 0.001$ and the above procedure is repeated until the converged results are obtained within a tolerance limit of 10^{-7} . All the computations are done in the Matlab software.

5 Results and Discussion

Before analyzing the numerical computation for the present problem with various values of the parameters involved such as suction parameter S , unsteadiness

parameter A , Prandtl number Pr , radiation parameter R and power-law exponent n , we firstly discuss about previously published analytical result of Miklavcic and Wang⁹, who gave analytical solution for viscous flow due to a shrinking sheet in the presence of uniform suction for steady state condition, i.e., $\lambda = 0$ as $f(\eta) = S^2/(S + \eta)$, which was valid for $S = \sqrt{6/(2m - 1)}$ (where m is the shrinking parameter with $m = 1$ for sheet shrinks in x - direction only while $m = 2$ for axisymmetric shrinking sheet). In the case axisymmetric shrinking sheet, he noticed that for $S < (S_0 = 1.31175869)$ there exist no solution and for $S > (S_1 = 1.4238297 \approx \sqrt{2})$ there exists only one solution, i.e., unique solution while dual solutions exist for $S_0 < S < S_1$.

Now, for a comparative analysis with Miklavcic and Wang⁹, we have plotted the Fig. 2 of the skin friction coefficient $f''(0)$ against S for several values of A . It is noticed that for $A = 0$, i.e., for steady-state condition, there exists no similarity solution for $S < 1.3117 \approx S_0$ and consequently, there exist the dual solutions for all values of $S \geq 1.3117$. Hence, in the steady-state condition, the present numerical investigation explores the conditions of either no solution or dual solutions. In other words we can say that in the present numerical investigation there exists only dual solution in the both certain ranges of existence of unique as well as dual solutions of suction parameter S given by Miklavcic and Wang⁹, which is also a new result for us. Further, it is also observed that in the case of first solutions (upper branch), the skin friction coefficient $f''(0)$ increases for increasing values of S and A . While in the case of

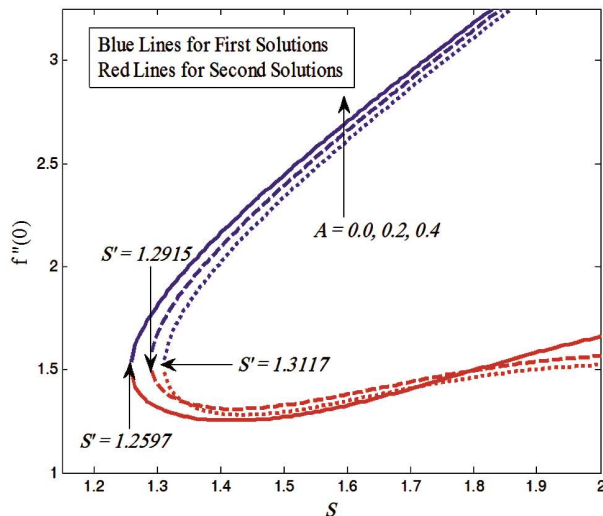


Fig. 2 — Variations of $f''(0)$ with S for various values of A .

the second solution (lower branch), for increasing values of S it initially decreases then it starts to increase and at the end it again decreases. With increase of A , the $f''(0)$ decreases for very small values S and for large values of S it increases.

The range of S for the existence and the non-existence of the dual solutions for different values of A is given in Table 1. It can be easily seen from Fig. 2 and Table 1 that with an increment in the values of A , the range of S where the similarity solutions exist, also increases. This is also a new solution emerged from the numerical investigation. Here, the enhancement in the existing range of similarity solution due to increment in unsteadiness condition is physically realistic. For increasing values of unsteadiness parameter, the generation of the vorticity at the sheet is slightly reduced and therefore, to contain the vorticity within the boundary layer the required adequate suction can be taken smaller than to take in the case of steady-state. Hence, the similarity solution is possible for smaller values of S as well in the presence of the unsteady-state condition.

The velocity profiles $f'(\eta)$ for several values of S in the presence of unsteady shrinking sheet are depicted in Fig. 3. It is noticed that for increasing

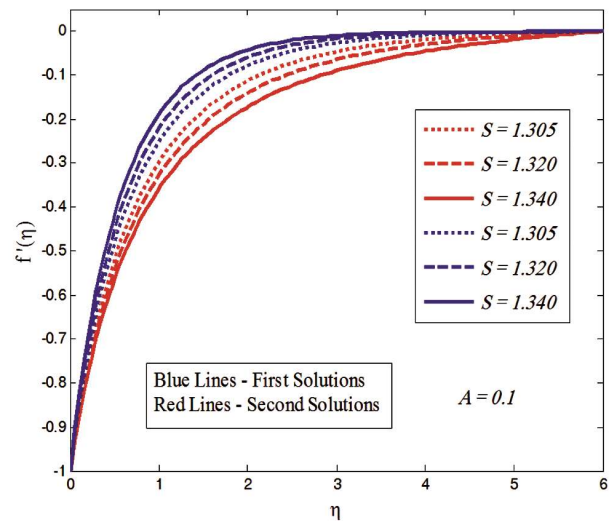


Fig. 3 — Velocity profile $f'(\eta)$ for various values of S .

Table 1 — Ranges of S for the existence and non-existence of dual solutions for several values of A .

A	Existence of dual solution	Non-existence of solution
0	$S \geq 1.3117$	$S < 1.3117$
0.1	$S \geq 1.3050$	$S < 1.3050$
0.2	$S \geq 1.2915$	$S < 1.2915$
0.3	$S \geq 1.2776$	$S < 1.2776$
0.4	$S \geq 1.2597$	$S < 1.2597$
0.5	$S \geq 1.2352$	$S < 1.2352$

values of S , the velocity profile increases for the first solution while decreases for the second solution case. The curves of temperature profile $\theta(\eta)$ for several values of S in the presence of unsteady shrinking sheet with radiation effect are plotted in Fig. 4. It is noticed that for increasing values of S , the temperature at a point decreases for the first solution while increases for the second solution case. Therefore, we can say that with the increasing values of suction parameter S , the velocity as well as thermal boundary layer thickness both decreases in the case of first solution while in the case second solution both increases. The velocity profiles $f'(\eta)$ for several values of A in the presence of suction are displayed in Fig. 5. It is noticed that with increase of A , the

velocity profile increases for the first solution while for the second solution it behaves oppositely, i.e., it decreases. Figure 6 exhibits that with increase of A , the temperature at a point decreases for the first solution while for the second solution it decreases near the sheet but after a certain distance normal to the sheet it increases. Figure 7 exhibits the temperature profile for various values of Pr in the presence of suction over an unsteady shrinking sheet. It is found that the temperature profile as well as thermal boundary layer thickness decreases with increasing values of Pr for both the first and second solution cases. The effects of radiation parameter R on the temperature profile are shown in Fig. 8. It is noticed from that for the both solutions, the

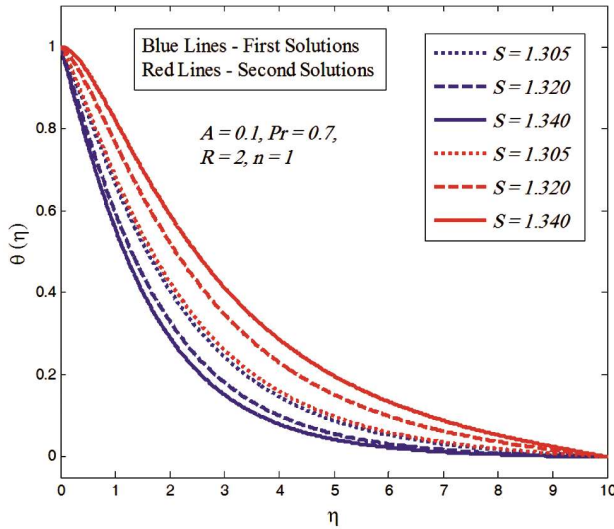


Fig. 4 — Temperature profile for various values of S .

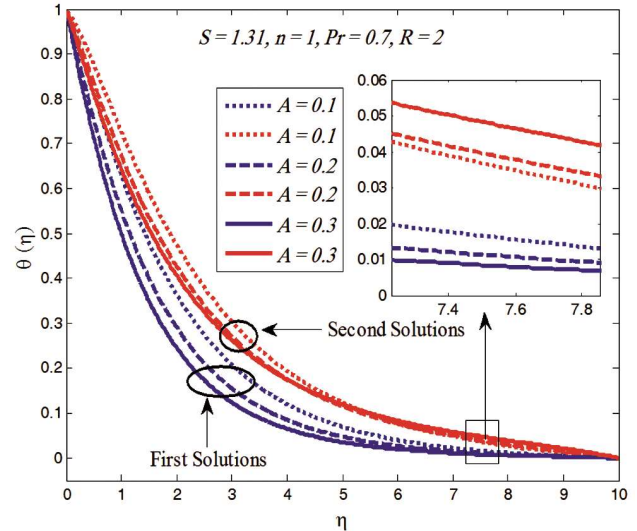


Fig. 6 — Temperature profile for various values of A .

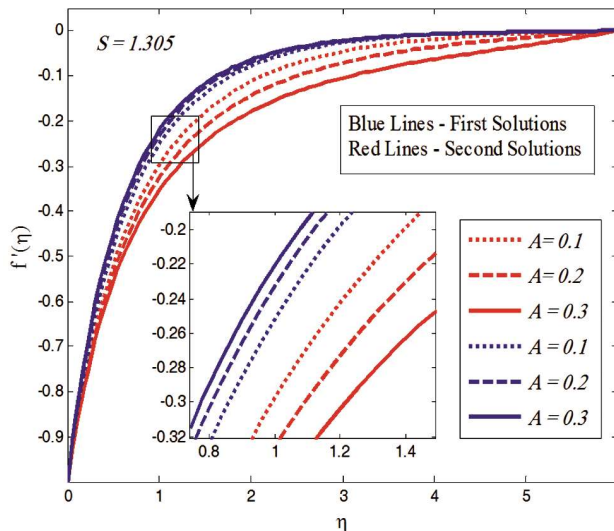


Fig. 5 — Velocity profile $f'(\eta)$ for various values of A .

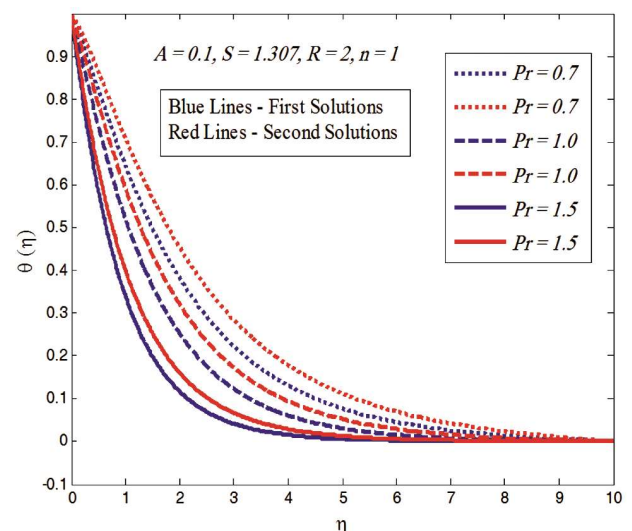


Fig. 7 — Temperature profile for various values of Pr .

temperature as well as the thermal boundary layer thickness decreases as the parameter R increases. Now the effect of power-law exponent n on the temperature profile is displayed in Fig. 9. It is observed that as the values of n increases, the thermal boundary layer thickness as well as temperature profile increases very fastly near the sheet and for large values of η , the temperature profile is vanishes as expected. Also, from all the figures of temperature profiles it is evident to conclude that the thermal boundary layer thickness for the second solution is higher than that of first solution case.

Now, the curves for the rate of heat transfer at the sheet or the local Nusselt number, i.e., $-\theta'(0)$ with S for various values of unsteadiness parameter A ,

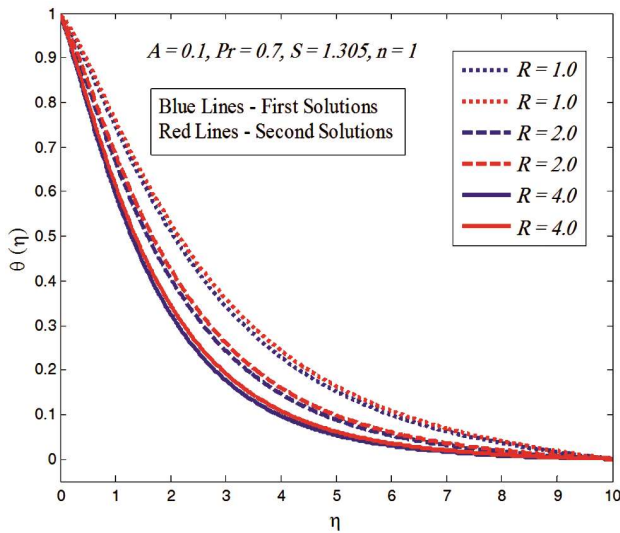


Fig. 8 — Temperature profile for various values of R .

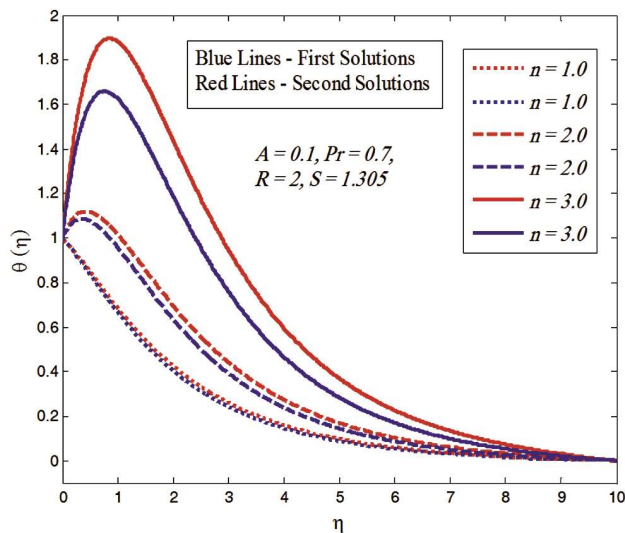


Fig. 9 — Temperature profile for various values of n .

Prandtl number Pr , radiation parameter R and power-law exponent n are given in Figs 10-13, respectively. It is seen from Fig. 10 that with increase of A , $-\theta'(0)$ increases for both the cases of first solution and second solution at a certain value of S . Figures 11-12 exhibit that for increasing values of Pr and R , $-\theta'(0)$ increases in the case of first solution while in second solution case, it decreases. Further, Fig. 13 exhibits that $-\theta'(0)$ decreases with increasing values of n in both the cases of first and second solutions. Moreover, from all these figures it can be easily seen that with increasing values of S , $-\theta'(0)$ increases in the case of first solution, while for second solution case it decreases.

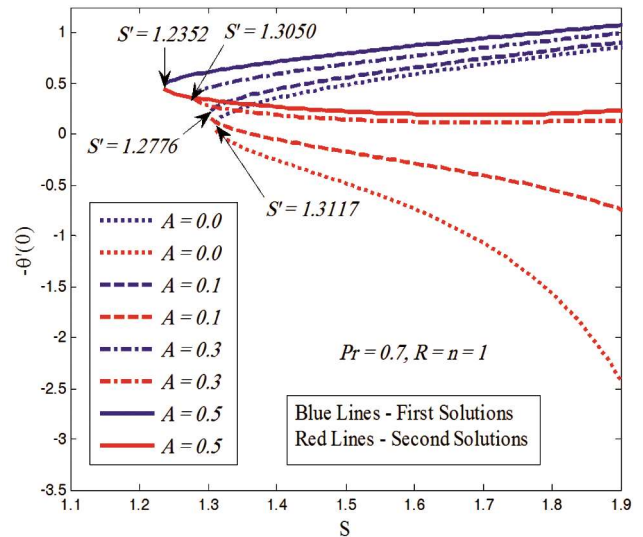


Fig. 10 — $-\theta'(0)$ with S for various values of A .

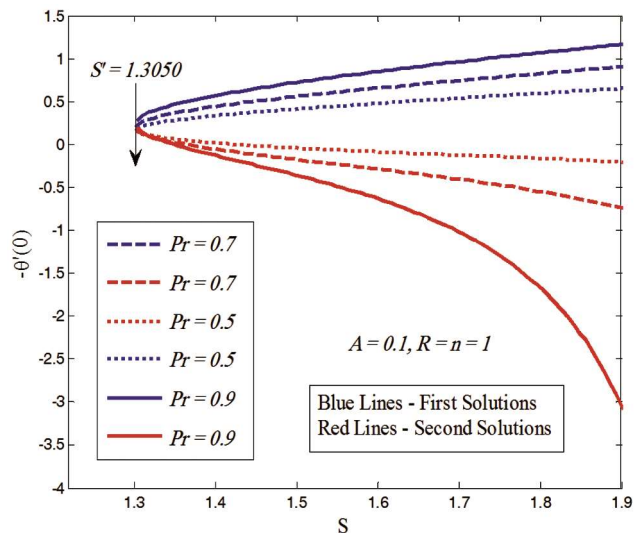


Fig. 11 — $-\theta'(0)$ with S for various values of Pr .

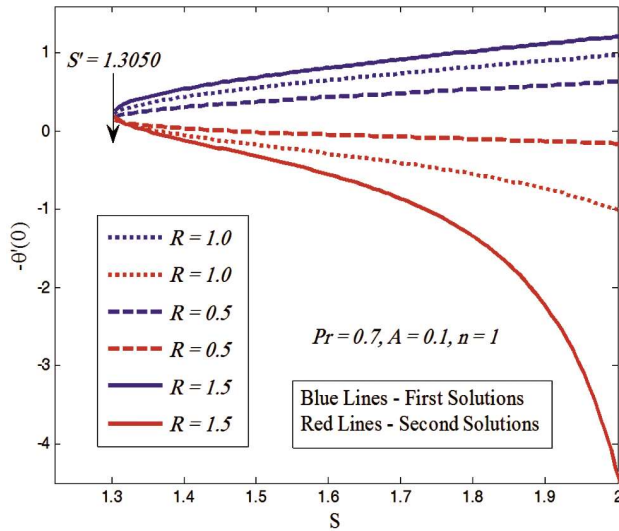


Fig. 12 — $-\theta'(0)$ with S for various values of R .

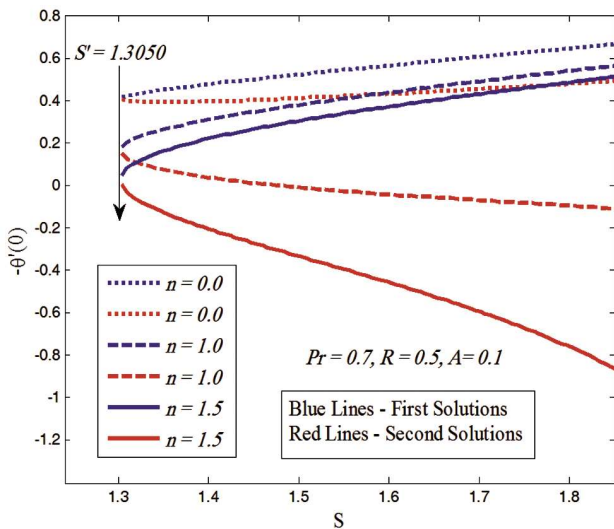


Fig. 13 — $-\theta'(0)$ with S for various values of n .

6 Conclusions

The objective of the present work is to analyze the effects of radiation parameter on unsteady three-dimensional boundary layer flow and heat transfer due to a permeable axisymmetric shrinking sheet with suction and power-law distribution of surface temperature. The set of nonlinear ordinary differential equations is solved numerically using Runge- Kutta fourth order algorithm with the shooting technique. Numerically it is observed that with the increase of unsteadiness parameter A , the certain range of the suction parameter S where the similarity solution of dual type exists, increases. With increase of suction and unsteadiness parameter, the skin friction coefficient increases in the case of first solution, while

for the second solution it gives fluctuating nature. The further investigation explores that the thermal boundary layer thickness of second solution case is higher than that of first solution case. Finally, the rate of heat transfer at the sheet increases with increase of unsteadiness parameter, Prandtl number, radiation parameter and suction parameter, while decreases with increase of power-law exponent parameter for the first solution case. On the other hand, i.e., for second solution case, it increases with increase of unsteadiness parameter while decreases with increase of Prandtl number, radiation parameter, suction parameter and power-law exponent parameter.

Acknowledgement

This work has been carried out with the financial support of CSIR, India in the form of Senior Research Fellowship under research scheme no. 09/149(0593)/2011-EMR-I awarded to the author (Dinesh Rajotia).

References

- 1 Crane L J, *Z Angew Math Phys*, 21 (1970) 645.
- 2 Gupta P S & Gupta A S, *Can J Chem Eng*, 55 (1977) 744.
- 3 Wang C Y, *Phys Fluids*, 27(8) (1984) 1915.
- 4 Ariel P D, *ZAMM*, 83 (2003) 844.
- 5 Elbashbeshy E M A, Emam T G & Wahed M S A, *Int J Energy Technol*, 3 (2011) 1.
- 6 Jat R N, Saxena V & Rajotia D, *Indian J Pure Appl Phys*, 51 (2013) 683.
- 7 Jat R N, Chand G & Rajotia D, *Therm Energy Power Eng*, 3(1) (2014) 191.
- 8 Wang C Y, *Appl Math*, 48 (1990) 601.
- 9 Miklavcic M & Wang C Y, *Appl Math*, 64 (2006) 283.
- 10 Wang C Y, *Int J Non-Linear Mech*, 43 (2008) 377.
- 11 Muhaimin R K & Khamis A B, *Appl Math Mech*, 29 (2008) 1309.
- 12 Hayat T, Abbas Z, Javed T & Sajid M, *Chaos Solitons Fractals*, 39 (2009) 1615.
- 13 Fang T & Zhang J, *Acta Mechanica*, 209 (2010) 325.
- 14 Bhattacharyya K, *Front Chem Sci Eng*, 5(3) (2011) 376.
- 15 Bhattacharyya K & Layek G C, *Int J Heat Mass Transfer*, 54 (2011) 302.
- 16 Rajotia D & Jat R N, *Chin Phys B*, 23 (2014) 074701.
- 17 Jat R N & Rajotia D, *Indian J Pure Appl Phys*, 52(2) (2014) 79.
- 18 Ghosh S, Mukhopadhyay S & Varjavelu K, *Alex Eng J*, 55 (2016) 1835.
- 19 Bhattacharyya K, Uddin M S & Layek G C, *Alex Eng J*, 55 (2016) 1703.
- 20 Haq R, Rajotia D & Noor N F M, *Eur Phys J E*, 39(3) (2016) 1.
- 21 Ghosh S & Mukhopadhyay S, *Int J Comput Meth Eng Sci Mech*, 18 (2017) 309.
- 22 Devi S, Takhar H S & Nath G, *Int J Heat Mass Transfer*, 29 (1986) 1996.
- 23 Mukhopadhyay S & Andersson H I, *Heat Mass Transfer*, 45 (2009) 1447.

- 24 Abd El-Aziz M, *Int Commun Heat Mass Transfer*, 36 (2009) 521.
- 25 Fang T, Zhang J & Yao S S, *Chin Phys Lett*, 26 (2009) 014703.
- 26 Bachok N, Ishak A & Pop I, *Appl Math Mech*, 31 (2010) 1421.
- 27 Chamkha A J, Aly A M & Mansour M A, *Chem Eng Commun*, 197 (2010) 846.
- 28 Ullah I, Bhattacharyya K, Shafie S & Khan I, *PLOS One*, 11 (2016) 1.
- 29 Aurangzaib, Bhattacharyya K & Shafie S, *Alex Eng J*, 55 (2016) 1285.
- 30 Brewster M Q, *Thermal radiative transfer properties*, (John Wiley and Sons: New York), 1972.